Separation Science and Technology
Publication details, including instructions for authors and subscription information:
http://www.informaworld.com/smpp/title~content=t713708471

Adsorption of anilines and cresols on NaX and different cation exchanged zeolites (equilibrium, kinetic, and IR investigations)

E. Titus[a]; A. K. Kalkar[a]; V. G. Gaikar[b]
[a] Applied Physics Division, Department of Chemical Technology, University of Mumbai, Matunga, Mumbai-400019, India [b] Chemical Engineering Division, Department of Chemical Technology, University of Mumbai, Matunga, Mumbai-400019, India

Online publication date: 25 April 2002

To cite this Article Titus, E. , Kalkar, A. K. and Gaikar, V. G.(2002) 'Adsorption of anilines and cresols on NaX and different cation exchanged zeolites (equilibrium, kinetic, and IR investigations)', Separation Science and Technology, 37: 1, 105 — 125
To link to this Article: DOI: 10.1081/SS-120000324
URL: http://dx.doi.org/10.1081/SS-120000324

SEPARATION SCIENCE AND TECHNOLOGY, 37(1), 105–125 (2002)

ADSORPTION OF ANILINES AND CRESOLS ON NaX AND DIFFERENT CATION EXCHANGED ZEOLITES (EQUILIBRIUM, KINETIC, AND IR INVESTIGATIONS)

E. Titus,[1] A. K. Kalkar,[1,*] and V. G. Gaikar[2]

[1]Applied Physics Division and
[2]Chemical Engineering Division, Department of Chemical Technology, University of Mumbai, Matunga, Mumbai-400019, India

ABSTRACT

The equilibrium isotherms and the rate of adsorption have been measured for anilines and cresols on different zeolites by the usual gravimetric method using Microforce balance system. The adsorption isotherms of different anilines on NaX and different exchanged zeolites were fitted in Langmuir, Nitta, and virial isotherms and various adsorption parameters were calculated. Diffusivity studies show that the rate of adsorption depends on the diameter of the molecule and the channel diameter. Diffusivities were observed to be concentration-independent and closely consistent with the Arrhenius relationship with activation energies as high as 96.6 kJ/mol. The infrared analysis of the induced bands of anilines and cresols on zeolites shows some additional bands related to N–H and O–H in anilines and cresols. The shift in these bands with respect to aniline and cresol spectra indicates the

*Corresponding author.

specific adsorption. Major shifts of the peaks are due to the lone pair–Lewis acid site interaction.

INTRODUCTION

The role of adsorption and diffusion of molecules within the pores of zeolites is important for shape selectivity and hence for separation process (1–5). The adsorption isotherms are useful in the estimation of interaction between the adsorbate and the adsorbent (6). The estimation of different adsorption parameters is important in the tailoring of zeolite adsorption characteristics in terms of size selectivity or the selectivity caused by interactions including cation exchange. The advent of laser excitation and the introduction of Fourier Transform instruments with on-line computer capability and its high sensitivity, have made it possible to obtain information about the adsorbed species in spite of the too weak signals (7).

The adsorption of various hydrocarbons on several common zeolites has been studied in detail by many authors (8–13). But very few attempts have been made to correlate the equilibrium and kinetic studies with IR studies (14).

In this paper, we report the results of detailed experimental study of equilibrium, kinetic, and IR investigation of adsorption of anilines and cresols on NaX and different cation exchanged zeolites, viz, KX, CaX, BaX.

N-Methylation of aniline gives a mixture of *N*-methyl aniline (NMA) and *N*,*N*-dimethyl aniline (DMA) along with the unreacted aniline. These are important intermediates in the dye, pharmaceutical, and rubber industries. Although aniline, which boils at 182°C, can be removed by distillation, NMA and DMA are liquids with boiling points of 195.6 and 193°C, respectively and they cannot be separated readily by fractional distillation. Even removal of traces of aniline is difficult by distillation. Alkyl phenols also form an important class of chemicals having a wide range of applications in pharmaceutical, insecticide, and flavor industries. (The boiling points of *p*-cresol, *m*-cresol, and 2,6-xylenol are 201.94, 202.23, and 201.03°C, respectively). Several reactive separation processes such as dissociation extraction, reactive crystallization and reactive distillation in presence of amines, etc., have been proposed for the separation and purification of these mixtures which are efficient but costly methods. Adsorptive separation is an alternative for the separation of above-mentioned compounds.

The channel diameter of NaX zeolite is 7.4 Å. The size of the anilines and cresols are comparable with the channel diameter of the zeolite and they are accessible to the zeolite channel. Therefore, preferential selection of one

MARCEL DEKKER, INC.
270 Madison Avenue, New York, New York 10016

molecule over other is expected. The cresols and anilines are polar molecules and therefore interaction of these molecules with the cations was expected.

MATERIALS AND EXPERIMENTAL PROCEDURE

N-methylaniline with a purity of 98.0% was supplied by SISCO Research Laboratories Pvt. Ltd. Aniline, *N*,*N*-dimethyl aniline, *p*-cresol, *m*-cresol, and *o*-cresol were supplied by S D Fine Chemicals, Mumbai. Molecular sieves 13X in the form of pellets ($1.5 \times 2.5\,mm^2$) manufactured by ACC Ltd were supplied by S D Fine Chemicals, Mumbai.

KX, CaX, and BaX zeolites were prepared by exchanging NaX zeolite with the salt solution repeatedly. A small amount (50 mL) of 2 *M* KOH, $CaCl_2$, and $BaCl_2$ solutions were treated with 25 g of NaX zeolite in a round bottom flask at room temperature for 6 hr. Then, the exchanged zeolites were filtered, washed, and dried.

The studies of equilibrium and rate of adsorption were performed using Microforce balance system (Ci electronic, U.K) attached to vacuum system and data acquisition system. The data acquisition system provides storage of pressure and sample weight data at any desired time intervals. For IR studies the powder zeolite samples were pressed (Pressure 3 tons) in the form of self supported pellets (2 mg). The pellets were activated at 450°C and then placed in the evacuation chamber to remove the residual moisture. The adsorption experiments were carried out and pellets were analyzed in the IR beam. The analysis was done in Bruker spectrophotometer with 256 scanning and resolution $4\,cm^{-1}$.

RESULTS AND DISCUSSION

Equilibrium Studies

The adsorption isotherms of different anilines on NaX and different exchanged zeolites were fitted in Langmuir, Nitta, and virial isotherms and various adsorption parameters were calculated. The most suitable isotherm was the Langmuir isotherm and the equilibrium constant and loading capacity were obtained from the linear form of this isotherm.

Figure 1 shows the isotherm for different anilines on NaX zeolite at 303K. The isotherms were concave to the *X*-axis, which shows the interaction between the aniline and the zeolite. The adsorption increases with the increase in pressure and saturation is reached at the equilibrium pressure. Equilibrium constant is a measure of the interaction between the adsorbate and the adsorption site. At a particular temperature, the equilibrium constant decreases in the order:

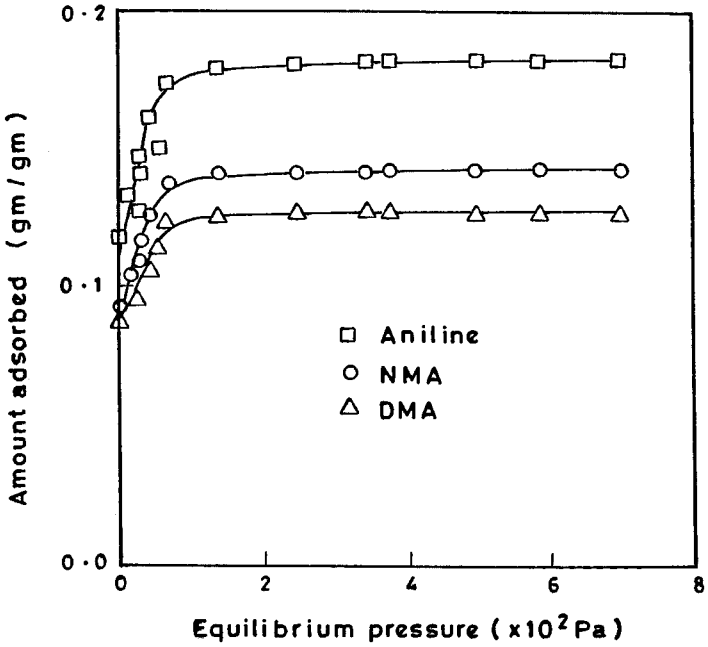

Figure 1. Adsorption isotherms of aniline on NaX zeolite at 303K.

N,*N*-dimethylaniline $(36.7\times10^{-2}\,\mathrm{Pa}^{-1}) > N$-methylaniline $(29.7\times10^{-2}\,\mathrm{Pa}^{-1})$ > aniline $(26.8\times10^{-2}\,\mathrm{Pa}^{-1})$. The adsorption of anilines into zeolites is due to the interaction between the lone pair of electrons in the nitrogen atom of the aniline and Lewis acid site.

The electrons of the hydrogen atom attached to nitrogen in aniline are pulled by the electronegative nitrogen atom and it develops a partial negative charge. When the aniline comes into contact with the zeolite, the nitrogen atom tries to balance the negative charge by donating electrons to the Lewis acid site of the zeolite. This is stabilized again by the electrons from the benzene ring by resonance. The charge density of different anilines obtained by quantum mechanical calculations from the molecular modeling Chem-X Software developed by Chemical Design Ltd., Oxon, England are in the order: DMA $(8.7\times10^{-19}\,\mathrm{C/\AA^3}) >$ NMA $(8.4\times10^{-19}\,\mathrm{C/\AA^3}) >$ Aniline $(8.2.\times10^{-19}\,\mathrm{C/\AA^3})$. The charge density of methyl substituted anilines is high due to the + inductive effect of the methyl group. The equilibrium constant increases with the increase in charge density because the partial negative charge on the nitrogen increases

MARCEL DEKKER, INC.
270 Madison Avenue, New York, New York 10016

with the increase in electron density and it tries to stabilize the negative charge by donating electrons to the zeolite.

For exchanged zeolite, the equilibrium constant was dependent on the strength of the cation electric field. The strength of the cation field is decided by the charge and the size of the cation. The equilibrium constant for divalent cation zeolites was higher than that of monovalent cation zeolite. The equilibrium constants for aniline on NaX and KX were 26.8×10^{-2} and $25.01\times10^{-2}\,Pa^{-1}$ and that of CaX and BaX zeolites were 43.9×10^{-2} and $42.0\times10^{-2}\,Pa^{-1}$. Among monovalent cation zeolites, the small difference in equilibrium constant is due to the difference in the size of the cations. When the size of the cation is small, it has higher charge density (the charge densities of Na^+, K^+, Ca^{2+}, and Ba^{2+} are 0.1392, 0.0752, 0.259, and $0.141\times10^{-19}\,C/Å^3$ and the electrostatic interaction between the adsorbate and the cation increases. Similarly, among divalent cation zeolites, the equilibrium constant was higher for CaX than BaX zeolite.

The adsorption capacities were also obtained from the linear form of the Langmuir isotherm. At a particular temperature, the adsorption capacity was in the decreasing order: aniline (1.96 mol/kg) > *N*-methyl aniline (1.33 mol/kg) > *N*,*N*-dimethyl aniline (1.07 mol/kg) (the kinetic diameters of aniline, *N*-methyl aniline, and *N*,*N*-dimethylaniline are 5.79, 7.15, and 7.23 Å respectively). The higher adsorption capacity of aniline is due to the linear and close packing of aniline inside the zeolite. However, with NMA and DMA, close packing of these solutes is not possible due to the steric repulsion of the CH_3 groups. This reduces the adsorption capacity. For cation exchanged zeolites the adsorption capacities were lesser for divalent cations compared with the monovalent cations. This was because of the higher number of cation sites in monovalent cation zeolites. The adsorption capacities for anilines on different exchanged zeolites are given in Table 1.

The experimental data were also fitted in Nitta isotherm. The fitting was done for different *n* values. The isotherm was most suitable when the value of *n* is one. So, the Nitta Model resembles the Langmuir model. Table 2 shows the first virial coefficient, *A*, and the second virial coefficient, *B* obtained from the virial equation of state model for adsorption of anilines on different zeolites. The *A* and *B* values were obtained by a least square method. The Henry's coefficients calculated from the first virial coefficient were in the order: *N*,*N*-dimethyl aniline > *N*-methylaniline > aniline, which correlate well with the equilibrium constants obtained from the Langmuir isotherm. The second virial coefficient was highest for aniline and was least for *N*,*N*-dimethyl aniline. The negative sign shows that the interaction is negative. For the two molecules to interact, a most stable distance exists where the interaction energy is minimum. If the molecules are small, the interaction energy will be attractive and with the increase in the diameter of the molecule the repulsive interaction become more significant. Here,

MARCEL DEKKER, INC.
270 Madison Avenue, New York, New York 10016

Table 1. Loading Capacities for Anilines on Different Cation Zeolites

Zeolite	Adsorbate	Adsorption Capacity (mol/kg)		
	Temperature (K)	297	303	313
NaX	Aniline	2.06	1.96	0.176
	N-Methyl aniline	1.42	1.33	1.23
	N,*N*-Dimethyl aniline	1.09	1.04	0.97
KX	Aniline	2.00	1.84	1.73
	N-Methyl aniline	1.42	1.38	1.28
	N,*N*-Dimethyl aniline	1.06	0.925	0.84
CaX	Aniline	1.62	1.58	1.51
	N-Methyl aniline	1.21	1.13	1.04
	N,*N*-Dimethyl aniline	0.925	0.85	0.80
BaX	Aniline	1.60	1.48	1.38
	N-Methyl aniline	1.19	1.08	0.109
	N,*N*-Dimethyl aniline	0.90	0.83	0.77

Table 2. Virial Coefficients for the Adsorption of Anilines on Different Cation Zeolites

Zeolite	Adsorbate	First Virial Coefficient ($mol/m^2\,Pa^{-1}$)	Second Virial Coefficient $(mol/m^2)^2Pa^{-1}$
NaX	Aniline	10.9	−0.054
	N-Methyl aniline	11.0	−0.046
	N,*N*-Dimethyl aniline	11.1	−0.31
KX	Aniline	10.1	−0.070
	N-Methyl aniline	10.3	−0.061
	N,*N*-Dimethyl aniline	10.9	−0.043
CaX	Aniline	10.6	−0.011
	N-Methyl aniline	11.4	−0.099
	N,*N*-Dimethyl aniline	12.2	−0.082
BaX	Aniline	10.3	−0.092
	N-Methyl aniline	10.9	−0.079
	N,*N*-Dimethyl aniline	12.1	−0.071

the size of the aniline is comparable with the pore size of the zeolite and so, the interaction is repulsive. The repulsive interaction is highest for aniline due to the close packing of aniline. The *C* values were negligible compared to *A* and *B* values.

In cation exchanged zeolites, Henry's constant obtained for divalent zeolites was higher than that of monovalent zeolites. Since Henry's coefficient signifies interaction between adsorbate and adsorbent, the interaction was more for divalent zeolites because of the stronger electrostatic field produced by them. Among monovalent zeolites, the *A* values were higher for sodium zeolite. This is due to the higher charge density of sodium cation compared with the potassium cation. Similarly, for divalent cation also the *A* value was higher for calcium zeolite having high cation charge density. For monovalent cations, the second virial coefficient was lesser for sodium than for potassium. Since the second virial coefficient signifies the interaction between the adsorbate molecules, the molecular interaction was inversely proportional to adsorbate–adsorbent interactions. The inverse effect of the molecular interaction was due to the strong cation adsorbent interaction. Similarly, for divalent cations, the molecular interactions reduced with increase in the cation adsorbent interaction.

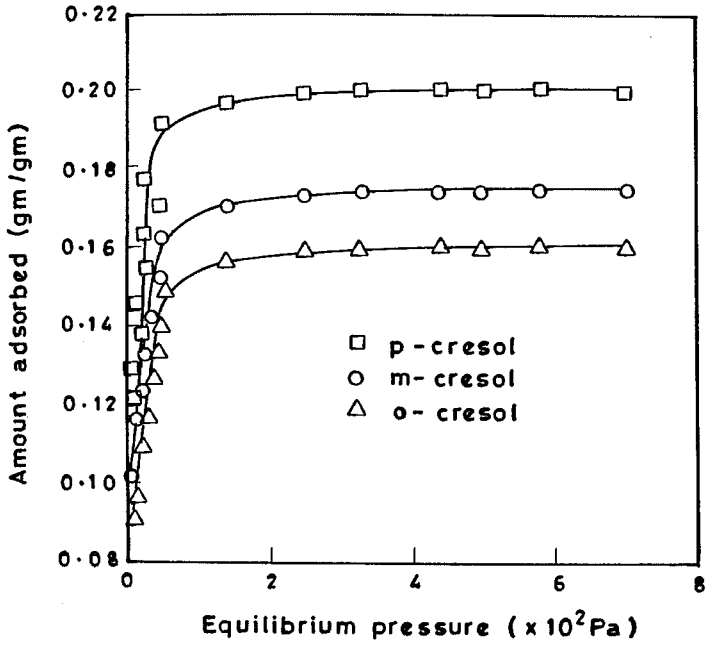

Figure 2. Adsorption isotherms of cresols on NaX zeolite at 303K.

MARCEL DEKKER, INC.
270 Madison Avenue, New York, New York 10016

Figure 2 shows the Langmuir adsorption isotherms of cresols on NaX at 303K. At room temperature, the equilibrium constants were in the order: *p*-cresol $(24.9\times10^{-2})^{-1}\mathrm{Pa}^{-1} > m$-cresol $(22.7\times10^{-2})^{-1}\mathrm{Pa}^{-1} > o$-cresol $(21.5\times10^{-2})^{-1}\mathrm{Pa}^{-1}$. The adsorption of cresols was due to the interaction between the lone pair of electrons in the oxygen atom of the cresols and the Lewis acid site of the zeolite and also due to the electrostatic interactions between the cation site and the cresols. Like anilines, for cresols also when there is lone pair electron interaction the charges are stabilized by the electrons from the benzene ring by resonance. The charge density of the three cresols is same (8.1×10^{-19} C/Å^3) because the functional group is same. However, the interaction was more in *p*-cresol because the charge on the carbon atom was stabilized by the methyl group. In *m*-cresol, the methyl group attached to the meta position was not taking part in stabilization and the interaction was less. In *o*-cresol, even though there is charge stabilization, the interaction was less due to the steric effect of the methyl group in the *o*-position. The adsorption capacity of cresols were in the order: *p*-cresol (1.87 mol/kg) > *m*-cresol (1.62 mol/kg) > *o*-cresol (1.5 mol/kg). The kinetic diameters of different cresols are — *p*-cresol = 5.8, *m*-cresol = 7.29, *o*-cresol = 7.31 Å. When cresols are adsorbed into zeolites, the cresol molecules occupy different sites. The adsorption capacity for *p*-cresol was high due to the linear packing of *p*-cresol in the sites. The functional groups and the methyl groups are in the opposite direction and the steric interaction between two adjacent adsorbed molecules was less. The steric interaction between the adjacent adsorbed molecules increases further in *m*-cresol and it was highest in *o*-cresol. The loading capacity values of cresols for cation exchanged zeolites are given in Table 3. Like anilines, for cresols also, the higher number of cations in monovalent cation zeolites was responsible for their high loading capacity on monovalent cation zeolites. Like anilines, for cresols also, the first virial coefficient was more significant than the second and the third virial coefficients. The virial coefficients obtained for different cresols on different zeolites are given in Table 4.

The effect of the temperature on the equilibrium constants can be obtained by using Vant Hoff's relation, which is given by (15)

$$\partial \ln(K_i)/\partial T = \Delta H_j/RT^2$$

Since heat of adsorption is a direct measure of the strength of the bonding between adsorbate and adsorbent it matches with the equilibrium constant. The heats of adsorption for different anilines and cresols are given in Table 5.

The information concerning the nature of an adsorbed species can be obtained from the analysis of the entropy of adsorption. The entropy can be calculated knowing the value of K and ΔH (16) (The Gibbs function, ΔG =

MARCEL DEKKER, INC.
270 Madison Avenue, New York, New York 10016

Table 3. Loading Capacities of Cresols on Different Cation Zeolites

Zeolite	Adsorbate	Adsorption Capacity (mol/kg)		
	Temperature (K)	297	303	313
NaX	*p*-Cresol	1.962	1.87	1.83
	m-Cresol	1.72	1.62	1.51
	o-Cresol	1.58	1.5	1.42
KX	*p*-Cresol	1.92	1.81	1.76
	m-Cresol	1.76	1.68	1.60
	o-Cresol	1.57	1.49	1.38
CaX	*p*-Cresol	1.46	1.36	1.27
	m-Cresol	1.22	1.12	1.055
	o-Cresol	1.20	1.11	1.00
BaX	*p*-Cresol	1.37	1.27	1.16
	m-Cresol	1.21	1.11	1.03
	o-Cresol	1.19	1.09	1.00

Table 4. Virial Coefficients for the Adsorption of Cresols on Different Cation Zeolites

Zeolite	Adsorbate	First Virial Coefficient $(mol/m^2)Pa^{-1}$	Second Virial Coefficient $(mol/m^2)^2Pa^{-1}$
NaX	*p*-Cresol	12.1	−0.0521
	m-Cresol	11.6	−0.0431
	o-Cresol	11.4	−0.0430
KX	*p*-Cresol	11.5	−0.0268
	m-Cresol	10.8	−0.0188
	o-Cresol	10.2	−0.0167
CaX	*p*-Cresol	13.2	−0.0983
	m-Cresol	12.8	−0.0911
	o-Cresol	12.4	−0.0861
BaX	*p*-Cresol	12.7	−0.0791
	m-Cresol	12.5	−0.0683
	o-Cresol	12.3	−0.0658

MARCEL DEKKER, INC.
270 Madison Avenue, New York, New York 10016

Table 5. Heat of Adsorption for Anilines and Cresols on Different Zeolites

	Heat of Adsorption (kJ/mol)			
Adsorbates	NaX	KX	CaX	BaX
Aniline	10.08	7.56	17.43	16.88
NMA	10.92	8.82	18.48	17.43
DMA	12.18	10.66	20.58	19.74
p-Cresol	10.08	8.19	20.16	19.32
m-Cresol	8.82	7.03	18.48	16.38
o-Cresol	8.40	6.636	18.06	15.54

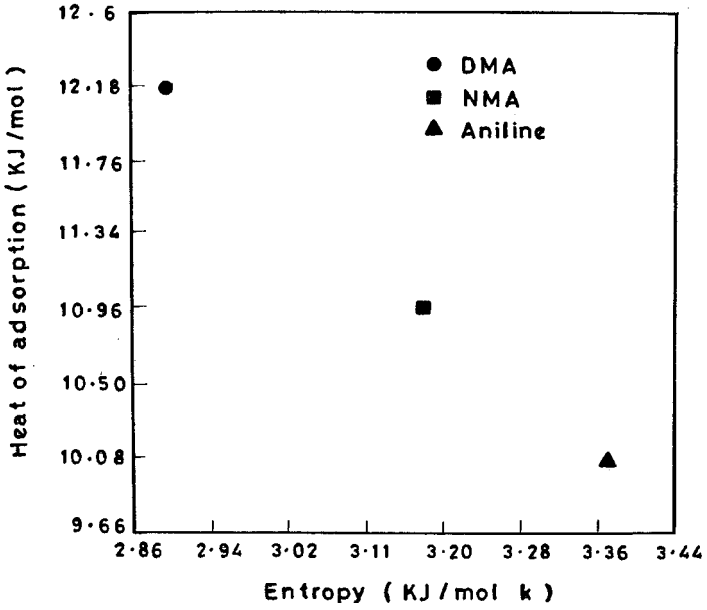

Figure 3. The plot of the entropy vs. heat of adsorption of anilines on NaX zeolite.

MARCEL DEKKER, INC.
270 Madison Avenue, New York, New York 10016

$\Delta H - T\Delta S$. The non-zero value of S indicates the specific interaction.) The plot of entropy vs. heat of adsorption for different anilines is shown in Fig. 3.

Diffusion Studies

The zeolite crystals are essentially spherical and uniform in size, so the diffusion is assumed to follow the Fick's equation. By taking into account the adsorption also, the mathematical solution to the diffusional process, which has been assumed to be Fickian under these conditions is (17)

$$\frac{M_t}{M_\infty} = 1 - \frac{6}{\pi^2}\sum_1^\infty \frac{1}{n^2}\exp(-n^2\pi^2 D' t/R^2)$$

where M_t is the amount adsorbed with respect to time. M_∞ is the saturation amount while $D' = D/(1 + K_a)$ where D is the diffusivity, R is the crystal radius, and K_a is the adsorption constant obtained from the linear portion of the Langmuir isotherm. The diffusivities were in the order: aniline > *N*-methylaniline > *N*,*N*-dimethylaniline.

Diffusion of anilines through the zeolite is affected by the interaction between the anilines and the zeolite channel wall and by the interaction of the anilines with the adsorption site. The interaction of anilines with the zeolite adsorption site follows the order: DMA > NMA > aniline. (The diffusivities of aniline, NMA, and DMA on NaX zeolite at 303K are 5.52, 4.83, and 4.61×10^{-13} m^2/sec, respectively.) Since the size of the diffusing anilines is very close to the pore size, potential wells of the molecule and the atoms on the channel wall may overlap, influencing significantly the movement within the channel. Therefore, the diffusivity was least for DMA and was highest for aniline. In addition, the steric hindrance due to CH_3 group slows down diffusivity of substituted anilines. Figure 4 shows the uptake curves for aniline on different cation exchanged zeolites. The diffusivities for aniline on different exchanged zeolites are given in Table 6. The diffusion coefficients were higher for calcium and barium exchanged zeolites compared with sodium and potassium exchanged zeolites. The number of cations in the divalent cation zeolites was less than that of monovalent cation zeolites because one divalent cation can replace two monovalent cations. Therefore, the number of cations present in the channel was less for divalent cation zeolite. The effect of the cation size on diffusion is more pronounced for molecules with smaller kinetic diameter than for molecules with kinetic diameter comparable to the pore openings. So, the effect of cation size for the diffusion of aniline was more pronounced for aniline than for *N*-methylaniline and *N*,*N*-dimethylaniline. The sizes of Na^+ and K^+ are 1.96 and 2.66 Å, respectively. For the smaller molecules, blockage caused by the larger K cation

MARCEL DEKKER, INC.
270 Madison Avenue, New York, New York 10016

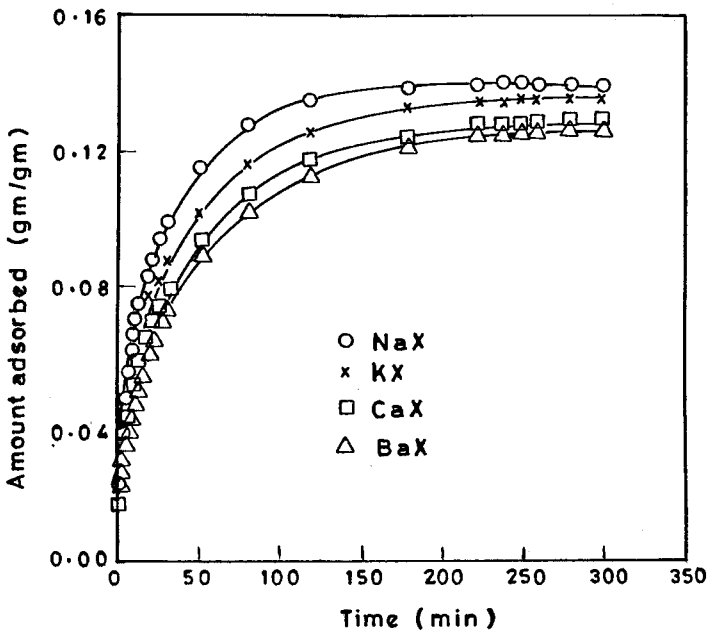

Figure 4. Uptake rate curves for aniline on different exchanged zeolites at temperature 303K.

slows down the diffusion process, while for large molecules having sizes comparable with the pore opening, the presence of cations of any size will constitute considerable blockage. Thus, the effect of cation size on the diffusion of these molecules is less pronounced. Due to the smaller size of sodium, the diffusivity was higher in sodium zeolite than in potassium zeolite. Similar is the case for divalent cations also (size of C^{2+} ions Ba^{2+} ions are 2.12 and 2.86 Å respectively).

Figure 5 shows the uptake curves for anilines on cation exchanged zeolites with different particle size. The time constants for diffusivity of anilines through zeolites of different particle size are also given in Table 6. For all the three anilines, the time constant for diffusion. D/r^2, was decreasing with the increase in particle size. By reducing the particle size, the number of pores of zeolite exposed per unit volume will be more, so the time constant for diffusion increases. However, absolute value of D remains the same, irrespective of the particle size. Since the D is decided only by intracrystalline pores, the size of the particle has no effect on the magnitude of D.

Table 6. Diffusivity of Aniline on Different Zeolites

	Particle Size (μm)	NaX $D\times10^{13}$ (m^2/sec)	NaX D/r^2 (sec^{-1})	KX $D\times10^{13}$ (m^2/sec)	KX D/r^2 (sec^{-1})	CaX $D\times10^{13}$ (m^2/sec)	CaX D/r^2 (sec^{-1})	BaX $D\times10^{13}$ (m^2/sec)	BaX D/r^2 (sec^{-1})
Aniline	75	5.52	5.89	4.9	5.31	8.12	8.53	6.1	6.52
	100	5.53	3.31	4.98	2.98	8.02	4.8	6.12	3.67
	150	5.55	1.47	4.96	1.32	8.08	2.13	6.15	1.69
NMA	75	4.83	5.13	4.61	4.92	5.18	5.51	5.08	5.34
	100	4.81	2.28	4.62	2.27	5.17	3.10	5.01	3.00
	150	4.85	1.01	4.67	1.23	5.23	1.37	4.99	1.33
DMA	75	4.61	4.9	4.46	4.81	4.92	4.41	4.83	4.11
	100	4.64	2.18	4.42	2.64	4.90	3.08	4.82	2.5
	150	4.60	1.0	4.41	1.18	4.88	1.26	4.76	1.21

MARCEL DEKKER, INC.
270 Madison Avenue, New York, New York 10016

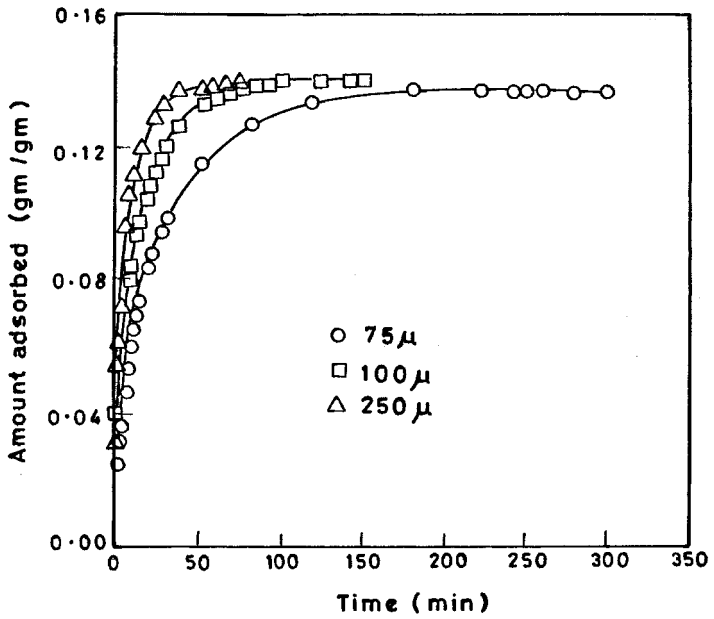

Figure 5. Uptake rate curves for anilines on NaX zeolite at temperature 303K.

Table 7. Variation of Diffusivity with Temperature for Anilines

Solute	Diffusivity $\times 10^{13}$ (m^2/sec)	Temperature (K)	Activation Energy (kJ/mol) (Experimental)	Activation Energy (kJ/mol) (Theoretical)
Aniline	4.13	293		
	5.52	303	63.64	59.22
	6.25	313		
NMA	3.61	293		
	4.83	303	70.56	72.24
	6.01	313		
DMA	3.2	293		
	4.6	303	96.18	93.24
	5.61	313		

Table 8. Diffusivity of Cresols on Zeolites of Different Particle Size

		NaX		KX		CaX		BaX	
	Particle Size (μm)	$D\times10^{13}$ m^2/s	D/r^2 (s^{-1})	$D\times10^{13}$ m^2/s	D/r^2 (s^{-1})	$D\times10^{13}$ M^2/s	D/r^2 (s^{-1})	$D\times10^{13}$ m^2/s	D/r^2 (s^{-1})
p-Cresol	75	5.33	5.89	4.81	5.14	6.93	7.39	6.28	6.68
	100	5.48	3.31	4.85	2.89	6.82	4.15	6.31	3.76
	150	5.5	1.49	4.90	1.28	6.91	1.84	6.2	1.67
m-Cresol	75	4.73	5.06	4.61	5.14	5.55	5.54	4.96	5.29
	100	4.78	2.85	4.7	2.89	5.46	3.12	4.89	2.97
	150	4.81	1.26	4.65	1.28	5.5	1.38	5.0	1.32
o-Cresol	75	4.58	4.88	4.31	4.6	5.12	5.46	4.79	5.1
	100	4.69	2.74	4.33	2.59	5.14	3.07	4.8	2.87
	150	4.62	1.21	4.35	1.15	5.17	1.36	4.75	1.27

MARCEL DEKKER, INC.
270 Madison Avenue, New York, New York 10016

The variation of diffusivity with temperature and the activation energy calculated by plotting $\ln D$ vs. $1/T$ for different anilines is given in Table 7. Among anilines, the activation energy was least for aniline and it was highest for *N*,*N*-dimethyl aniline. Therefore, aniline molecules could come out of the potential well faster. The diffusivities calculated for different cresols on NaX and exchanged zeolite are given in Table 8. The diffusivity was highest for *p*-cresol and it was almost same for *o*- and *m*-cresol. Due to the linear structure and small kinetic diameter (diameters of *p*-, *o*-, and *m*-cresols are 5.8, 7.29, and 7.31 Å), *p*-cresol diffuses faster. In *o*- and *m*-cresols, the steric hindrance due to the methyl group reduces their diffusivity. Like anilines, for cresols also, the diffusivity increases with temperature. The activation energies calculated for cresols are *p*-cresol = 68.04, *m*-cresol = 76.02, and *o*-cresol = 97.02 kJ/mol. The activation energy was lowest for *p*-cresol and therefore it could come out of the potential well faster.

IR Investigations

The replacement of silicon atom by aluminium atom produces a charge imbalance in zeolite and can be balanced by the addition of cations. The lone pair of electrons of oxygen and nitrogen atoms in the cresols and anilines can interact with the cations and produce a dipole moment change in associated bonds. The IR spectrum is expected to give information about such interaction between the lone pair electrons of anilines and cresols and adsorption sites.

The major peaks in the zeolite spectrum are due to OH stretching ($3480\,cm^{-1}$) vibration and deformation ($1600\,cm^{-1}$) of the water molecule. There is a band in $1000\,cm^{-1}$ region, which is due to Si–O–Si asymmetric stretching. There are four bands in $800–400\,cm^{-1}$ region, which are due to different lattice vibrations. The major peaks in aniline spectrum are due to N–H, C–N, and C–H bonds. The N–H bond shows both stretching and deformation bands. The N–H asymmetric and symmetric bands are at 3430, 3352, and $3212\,cm^{-1}$. The scissoring bands at 1601 and $1620\,cm^{-1}$ are due to N–H deformations. It also shows aryl C–H stretching bands at 3070,3035, and $3021\,cm^{-1}$. The band due to C–N is in the $1277\,cm^{-1}$ region. The major peaks of *N*-methyl aniline are due to N–H asymmetric stretching and deformations, aryl and methyl C–N bond, and aryl and methyl C–H bonds. In *N*,*N*-dimethyl aniline the major peaks are due to aryl C–N bond, methyl C–N bond, aryl C–H bond, and methyl C–H bond. Both aniline and *N*-methyl aniline contain N–H asymmetric bands and the shift in these bands due to adsorption is higher in the case of *N*-methyl aniline (Fig. 6). The electrons of the hydrogen atom attached to nitrogen in aniline are pulled by the electronegative nitrogen atom and it develops a partial negative change. But when the aniline come into contact with the zeolite,

MARCEL DEKKER, INC.
270 Madison Avenue, New York, New York 10016

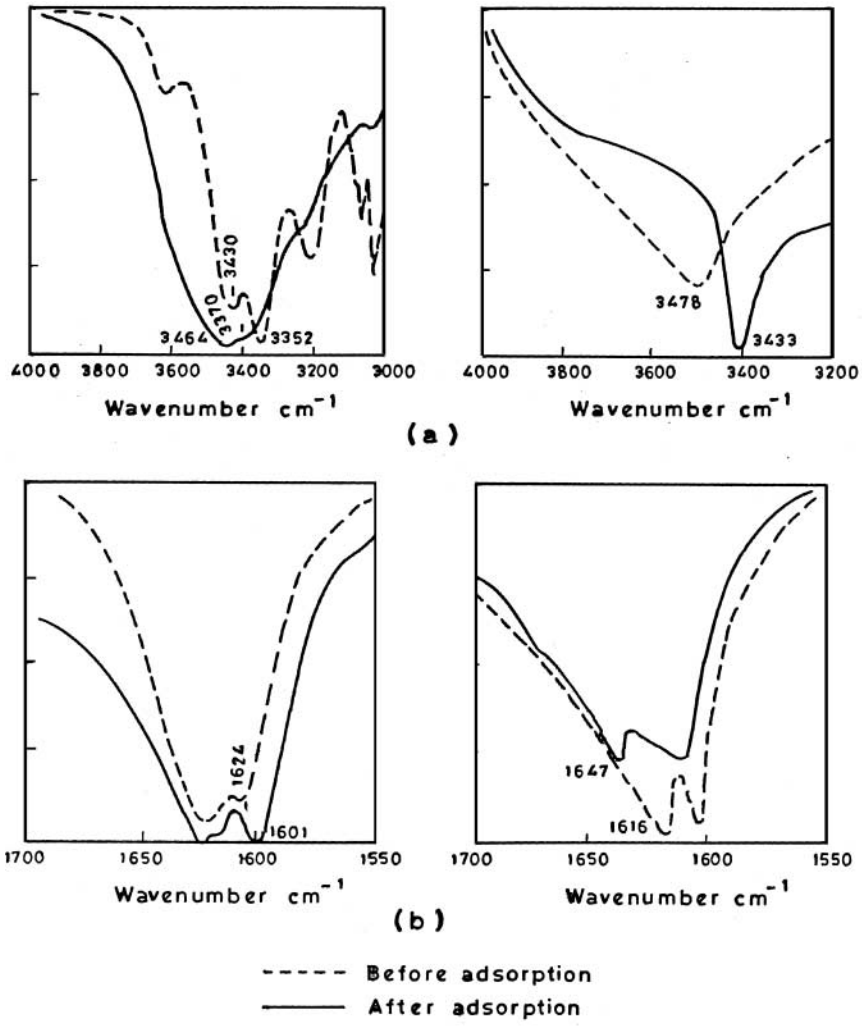

Figure 6. Frequency shift due to adsorption of (a) aniline, and (b) *N*-methyl aniline into zeolite.

the nitrogen atom tries to balance the negative charge by donating electrons to the Lewis acid site of the zeolite.

The charge density on nitrogen of methyl substituted anilines is high due to the + inductive effect of the methyl group. The charge density of different anilines at nitrogen are in the order: DMA > NMA > Aniline. The interaction

MARCEL DEKKER, INC.
270 Madison Avenue, New York, New York 10016

increases with the increase in charge density, because with the increase in electron density the partial negative charge on the nitrogen increases and it tries to stabilize the negative charge by donating electrons to the zeolite. Due to the +I effect of the methyl group, the electrons are released easily and increase the interaction. This results in the change in the dipole moment of the functional group. The aryl C–N bond and aryl C–H bond in aniline and NMA were however not affected by adsorption. This shows there is no direct interaction between the π electrons of the benzene ring and the zeolite. In the case of *N*-methyl aniline and aniline, the shifts in N–H band were higher for *N*-methyl aniline than aniline due to higher interaction in *N*-methyl aniline. Similarly the C–N band shift was higher for *N*,*N*-dimethyl aniline than *N*-methyl aniline, even though the shift was small for both *N*-methyl aniline and *N*,*N*-dimethyl aniline. The 800–400 cm^{-1} region bands were not affected by aniline adsorption. This is because the framework structure of the zeolites are very strong, so that there is no possible interaction of adsorbate with Si or Al in the framework.

The spectrum of *p*-cresol shows a major peak in the OH region (3338 cm^{-1} asymmetric stretching and 1616 cm^{-1} deformation). After adsorption, these peaks were shifted to 3433 and 1655 cm^{-1}, respectively. This is due to the interaction of the lone pair of electrons from oxygen with the framework cation site of the zeolite. Similarly, in the case of *m*-cresol, the 3329 cm^{-1} asymmetric stretching and 1616 cm^{-1} deformation bands were shifted to 3410 cm^{-1} and 1655 cm^{-1}. The shift in frequency was higher for *p*-cresol than for *m*-cresol (Fig. 7). This is due to the higher interaction of the *p*-cresol with the zeolite than the *m*-cresol. Due to the hyper conjugation effect of the methyl group, the carbon atom is stabilized and it easily releases lone pair of electron and increases interaction.

CONCLUSION

For the adsorption of anilines and cresols, the most suitable isotherm was the Langmuir isotherm. The perfect fitting of the adsorption data in Langmuir isotherm indicates the single site adsorption. Since the molecular diameter of anilines and cresols are smaller than the pore diameter of the zeolite channel, these molecules enter into the zeolites, but the difference in equilibrium constants is due to the difference in their electrostatic interactions.

The adsorption capacity was dependent on the kinetic diameter and the structure of the adsorbate. The Nitta model resembles the Langmuir model when the *n* value is equal to one. The deviation of the predicted values from the experimental value was higher for higher *n* values, which indicates single occupancy of the adsorbate. The magnitude of virial coefficient *A* obtained from the virial isotherm shows higher magnitude and the magnitude was low for *B*

Marcel Dekker, Inc.
270 Madison Avenue, New York, New York 10016

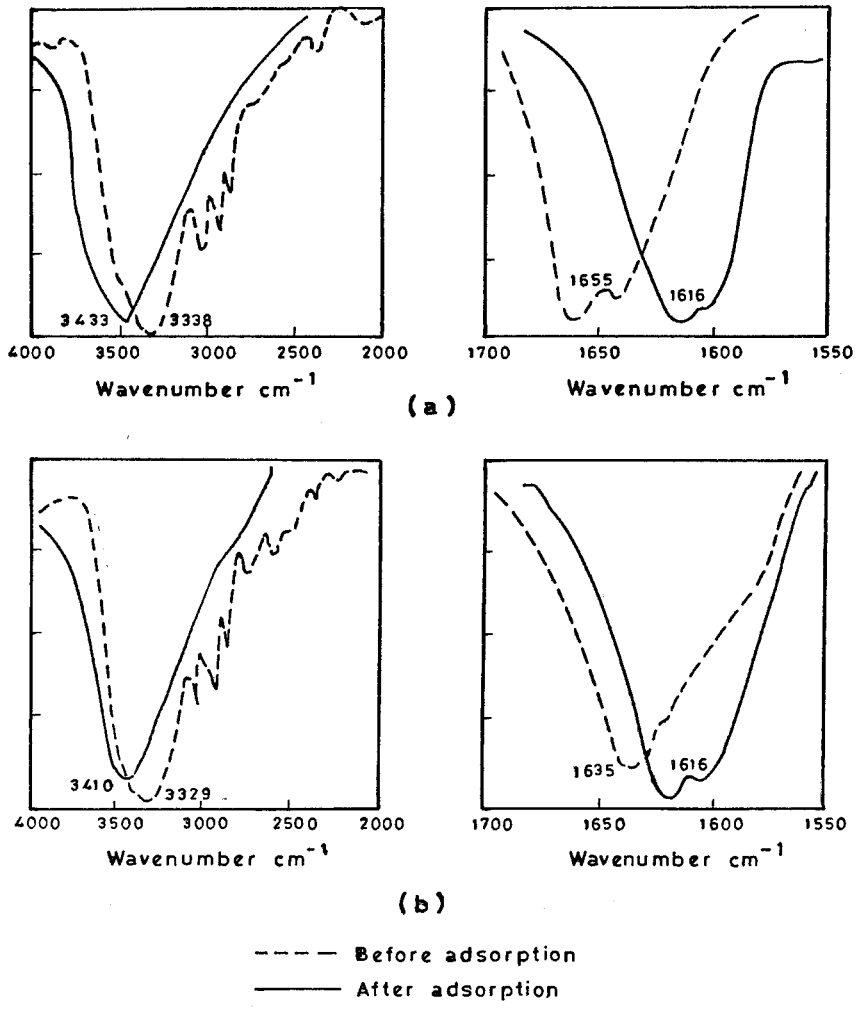

Figure 7. Frequency shift due to adsorption of (a) *p*-cresol, (b) *m*-cresol into zeolite.

value, which indicates the stronger interaction between the adsorbate and the adsorbent compared to adsorbate–adsorbent interactions.

Since diffusion in zeolite is due to the transport of a adsorbate molecule through the channel, it depends on the diameter of the channel and the diameter of the adsorbate molecule. The structure of the adsorbate also can affect the diffusion process. The diffusion coefficient of *p*-cresol and aniline were the

highest due to their smaller diameter and the linear structure. The diffusivity also increases with the increase in temperature. The effective diffusivity, however, remains same for all particle sizes but the apparent diffusivity (D/r^2) decreases with the increase in particle size. With the reduction in the particle size, more pores per unit volume are exposed and the overall diffusion becomes faster. The diffusivities were higher for divalent cation zeolite. As the number of cations is more in monovalent cations than in divalent cations, the cations blocking the zeolite channel are more in monovalent cation zeolite.

Adsorption studies using IR spectroscopy again confirms the interaction between the adsorbate and the adsorbent. The shift in the peaks due to adsorption shows the specific adsorption. Major shifts of the peaks are due to the lone pair–Lewis acid site interaction. Benzene ring interactions were not noticed.

REFERENCES

1. Anderson, R.; Forges, K.; Mole, T.; Rajadhyksha, R.A. Reactions on ZSM-5-type Zeolite Catalysis. J. Catal. **1979**, *58*, 114–130.
2. Barrer, R.M. Sorption in Porous Crystals: Equilibria and Their Interpretation. J. Chem. Technol. Biotechnol. **1981**, *31*, 71–85.
3. Barrer, R. M. Aluminosilicates Containing Sodalite and/or Carcrinite Cages Encapsulating Salts, US Patent 3674709, 1972.
4. Flanigen, E.M.; Bennet, J.M.; Grose, R.W.; Cohen, J.R.; Patton, R.L.; Kirchner, R.M.; Smith, J.V. Silicalite, a New Hydrophobic Crystalline Molecular Sieve. Nature (London) **1978**, *257*, 512.
5. Gaikar, V.G.; Mandal, T.K.; Kulkarni, R.G. Adsorptive Separations Using Zeolites: Separation of Substituted Anilines. Sep. Sci. Technol. **1996**, *31*, 259–270.
6. Breck, D.W. *Zeolite Molecular Sieves*; John Wiley: New York, 1974.
7. Kurlov, L.; Kanaausky, M.; Vladmir, B. Infrared Spectroscopic Study of the Interaction of Cations in Zeolites with Simple Molecular Probes, Part I. J. Chem. Soc. Faraday Trans. **1991**, *87*, 2675–2678.
8. Ruthven, D.M.; Bal, K. Kaul Assorption of Aromatic Hydrocarbons in NaX Zeolite: 2, Kinetics. Ind. Eng. Chem. Res. **1993**, *32*, 2053–2057.
9. Derouane, E.G.; Gabelica, Z. A Novel Effect of Shape Selectivity: Molecular Traffic Control in Zeolite ZSM-5. J. Catal. **1980**, *65*, 486–489.
10. Doelle, H.J.; Herring, J.; Rieckert, L. Sorption and Catalytic Reaction in Pentasil Zeolites 2: Influence of Preparation and Crystal Size on Equilibria and Kinetics. J. Catal. **1981**, *71*, 27–40.
11. Ma, Y.H.; Lin, Y.S. A Comparative Study of Adsorption and Diffusion of Vapor Alcohols and Alcohols from Aqueous Solutions in Silicalite. AIChE Symp. Ser. **1987**, *81*, 39.

MARCEL DEKKER, INC.
270 Madison Avenue, New York, New York 10016

12. Goddard, M.; Eic, M.; Ruthven, D.M. Diffusion of Benzene in NaX and Natural Faujasite. Zeolites **1988**, *8*, 327.
13. Eic, M.; Ruthven, D.M. A New Experimental Technique for Measurement of Intracrystalline Diffusivity. Zeolites **1988**, *8*, 41.
14. Jasra, R.V.; Choudary, N.V.; Rao, K.V.; Pandey, G.C.; Bhat, S.G.T. Far-infrared Spectroscopic Studies on Zeolites NaCaA. Chem. Phys. Lett. **1993**, *211*, 214–219.
15. Khodakov;; Yu, Andrew; Kustov, Andrew; Leonid, M.; Kazansky, B.; Vladmir, B.; Williams, B. Infrared Spectroscopic Study of the Interaction of Cations in Zeolites with Simple Molecular Probes. J. Chem. Soc., Faraday Trans. **1993**, *89*, 1393–1395.
16. Ruthven, D.M. *Principles of Adsorption and Adsorption Process*; Chap. 2, Wiley: New York, 1984.
17. Crank, *The Mathematics of Diffusion*; Claridon Press: Oxford, 1975.

Received April 2000
Revised February 2001

Request Permission or Order Reprints Instantly!